Neurobiology of Disease 201 (2024) 106671

Contents lists available at ScienceDirect

Neurobiology of Disease

journal homepage: www.elsevier.com/locate/ynbdi

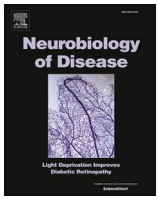

Dipeptidyl peptidase 4 deficiency improves survival after focal cerebral ischemia in mice and ameliorates microglia activation and specific inflammatory markers

Corinna Höfling [a,b], Philippa Donkersloot [a], Luise Ulrich [a], Sina Burghardt [a], Michael Opitz [a], Stefanie Geissler [c], Stephan Schilling [c,d], Holger Cynis [c,e], Dominik Michalski [b], Steffen Roßner [a,*]

[a] Paul Flechsig Institute for Brain Research, University of Leipzig, 04103 Leipzig, Germany
[b] Department of Neurology, University of Leipzig, 04103 Leipzig, Germany
[c] Fraunhofer Institute for Cell Therapy and Immunology, Department of Molecular Drug Design and Target Validation, 06120 Halle (Saale), Germany
[d] Anhalt University of Applied Sciences, Faculty of Applied Biosciences and Process Engineering, 06366 Köthen, Germany
[e] Junior Research Group "Immunomodulation in Pathophysiological Processes" Faculty of Medicine, Martin Luther University Halle-Wittenberg, Germany

ARTICLE INFO

Keywords:
Focal cerebral ischemia
Dipeptidyl peptidase 4
CCL2
Gliosis
Inflammation
Chemokines

ABSTRACT

Dipeptidyl peptidase 4 (DPP4; CD26) is involved in the regulation of various metabolic, immunological, and neurobiological processes in healthy individuals. Observations based on epidemiological data indicate that DPP4 inhibition by gliptins, typically used in patients with diabetes, may reduce the risk for cerebral ischemia and may also improve related outcomes. However, as DPP4 inhibitor application is neither complete nor specific for suppression of DPP4 enzymatic activity and DPP4 has non-enzymatic functions as well, the variety of consequences is a matter of debate. Therefore, we here used DPP4 knock-out (KO) mice to analyze the specific contribution of DPP4 to cellular, immunological, and functional consequences of experimental focal cerebral ischemia.

We observed a significantly higher survival rate of DPP4 KO mice after ischemia, which was accompanied by a lower abundance of the pro-inflammatory chemokine CCL2 and reduced activation of Iba1-positive microglia cells in brain tissue of DPP4 KO mice. In addition, after ischemia for 24 h to 72 h, decreased concentrations of CCL5 and CCL12 in plasma and of CCL17 in brain tissue of DPP4 KO mice were observed when compared to wild type mice. Other aspects analyzed, such as the functional Menzies score, astrocyte activation and chemokine levels in plasma and brain tissue were affected by ischemia but appeared to be unaffected by the DPP4 KO genotype.

Taken together, experimental ablation of DPP4 functions in mice improves survival and ameliorates aspects of cellular and molecular inflammation after focal cerebral ischemia.

1. Introduction

Stroke is the second most common cause of death in the European Union accounting for 440,000 deaths and affecting a total of 1.1 million inhabitants every year with annual stroke-associated direct and indirect costs of 45 billion € (for review see Wafa et al., 2020). Based on demographic developments of an aging population, the personal, health system and socio-economic burden is expected to increase dramatically (Feigin et al., 2023). Besides age, lifestyle factors such as physical exercise, diet and exposure to toxins including tobacco smoke and alcohol have a great impact on the likelihood of experiencing stroke.

Individual conditions such as arterial hypertension and type 2 diabetes pre-dispose to ischemic events (Sarikaya et al., 2015; Boehme et al., 2017). Following clinical guidelines, diabetes is currently treated by metformin, sodium-glucose cotransporter 2 (SGLT2) inhibitors, glucagon-like peptide-1 (GLP-1) receptor agonists, sulfonyl urea compounds, insulin and, more recently, by inhibitors of dipeptidyl peptidase-4 (DPP4; CD26) (Marguet et al., 2000; Sterrett et al., 2016;

Abbreviations: AD, Alzheimer's disease; BSA, bovine serum albumin; DAB, 3,3′-diaminobenzidine; DPP4, dipeptidyl peptidase 4; GLP-1, glucagon-like peptide-1; KO, knock-out; MCAO, middle cerebral artery occlusion; PBS, phosphate-buffered saline; TBS, tris-buffered saline; WT, wild type.

* Corresponding author at: Paul Flechsig Institute for Brain Research, Liebigstraße 19, 04103 Leipzig, Germany.
E-mail address: steffen.rossner@medizin.uni-leipzig.de (S. Roßner).

https://doi.org/10.1016/j.nbd.2024.106671
Received 17 June 2024; Received in revised form 11 September 2024; Accepted 15 September 2024
Available online 16 September 2024

McGovern et al., 2016). The latter are a group of compounds belonging to the chemical class of gliptins and prevent the degradation of GLP-1 and of glucose-dependent insulinotropic polypeptide (GIP), thus prolonging their biological half-life and thereby improving glucose tolerance. DPP4 inhibitors have a preferable safety profile, not causing hypoglycemia or increasing patient's weight (Deacon and Lebovitz, 2016; Lamos et al., 2019; Gilbert and Pratley, 2020). However, long-term consequences of DPP4 inhibition on the function of other physiological DPP4 substrates such as brain natriuretic peptide, substance P, neuropeptide Y and stromal cell-derived factor-1α (SDF-1α) should be considered (Elmansi et al., 2019).

In addition to metabolic regulation, DPP4 inhibitors also display anti-inflammatory profiles, which are partly due to the downregulation of pro-inflammatory chemokine expression. Such protective effects of DPP4 inhibition have been reported for liver steatosis (Shirakawa et al., 2011), glomerular injury and nephrotoxicity (Higashijima et al., 2015; Choi et al., 2017) and were related to diminished chemokine expression. Among the chemokines affected by DPP4 inhibition, CCL2 appears to play a central role (Choi et al., 2017; Ikedo et al., 2017; Hung et al., 2020).

After stroke, CCL2 expression is induced in microglia of the ischemic penumbra by factors released from degenerating astrocytes and neurons, thereby exerting CCL2 neurotoxicity mediated by CCR2 (Inose et al., 2015). Thus, DPP4 inhibition may reduce neuroinflammation and secondary neuronal cell death under ischemic conditions independent of its blood glucose-lowering effects. Indeed, there are a number of reports demonstrating beneficial effects of DPP4 inhibition in experimental stroke. For example, the DPP4 inhibitor Linagliptin reduced infarct volume and preserved neuronal survival in the penumbra in naïve and in diabetic mice after transient middle cerebral artery occlusion (MCAO) (Darsalia et al., 2013). Similar observations were made using the DPP4 inhibitor Alogliptin in normal mice subjected to stroke by the 3-vessel occlusion technique (Yang et al., 2013). Subsequently, Darsalia et al. (2014) demonstrated enhanced neural stem cell proliferation upon DPP4 inhibition in diabetic but not in naïve mice after stroke and Ma et al. (2015) reported ameliorated cognitive impairment and reduced brain atrophy upon Linagliptin treatment after transient cerebral ischemia. One underlying mechanism of the improved functional outcome after MCAO by DPP4 inhibition is the activation of the SDF-1α/CXCR4 pathway that could involve calcium homeostasis and Calpain activity (Chiazza et al., 2018). Also in rat models of MCAO (Röhnert et al., 2012) and of acute hemorrhagic stroke (Yip et al., 2020), the DPP4 inhibitor Sitagliptin reduced infarct volume and ameliorated neurological deficits.

Thus, DPP4 inhibition may contribute to stroke prevention, acute neuroprotection, and post-stroke recovery (for reviews see Darsalia et al., 2018, 2019). However, as DPP4 inhibitors such as Linagliptin act partly independent of GLP-1 receptor activation (Darsalia et al., 2019), there are a number of challenges associated with the use of these inhibitors. DPP4 exists as a membrane-bound 766 amino acid protein and as a soluble form lacking the transmembrane and intracellular domain (Mulvihill and Drucker, 2014). The vascular, immunological, and inflammatory activities of soluble DPP4 appear to be independent of its catalytic activity and the underlying mechanisms are difficult to uncover (Nauck et al., 2017). This is partly due to (i) the broad spectrum of DPP4 substrates involved in multiple cellular pathways, (ii) the low abundance of many DPP4 substrates, (iii) the lack of tools differentiating between intact and cleaved substrates, and (iv) the diverse regulation of biological activity upon cleavage by DPP4, resulting in inactivation or potentiation of biological activity (Ussher and Drucker, 2012, 2014; Mulvihill and Drucker, 2014).

To reveal a potential role of DPP4-specific enzymatic and non-enzymatic functions on the outcome of stroke, we here used DPP4 knock-out (KO) mice and a model of transient focal cerebral ischemia for comprehensive morphological, biochemical, and functional analyses.

2. Materials and methods

2.1. Animals

DPP4 KO mice (Dpp4tm1Nwa /Orl) were generated on C57BL/6J background by targeted deletion of DPP4 exon 1 and 2, resulting in inactivation of DPP4 expression (Marguet et al., 2000). DPP4 KO mice do not show phenotypic abnormalities such as motoric deficits or disturbances in eating, drinking and social behavior or fertility (Marguet et al., 2000). C57BL/6J wild type (WT) and DPP4 KO mice were maintained at the Fraunhofer Institute for Cell Therapy and Immunology, Halle, Germany, at 12 h day/12 h night cycles with food and water *ad libitum* in individually ventilated cages that contained nest building material. Genotyping of DPP4 KO mice was done in two separate PCRs discriminating between transgenic and WT alleles. Common sense primer was: 5′-GTA GAT GCA TCC AAT GAC CC-3′ in combination with antisense primer: 5'-ACA TTA GTT AGC GCA AGG CG-3′ for the WT allele (PCR product: 1100 bp) or antisense primer: 5'-ACT TGT GTA GCG CCA AGT GC-3′ for the transgenic allele (PCR product: 900 bp). The PCR protocol using Taq polymerase consisted of 3 min initial melting at 95 °C followed by 36 cycles of melting at 95 °C for 15 s, annealing at 60 °C for 15 s and elongation at 72 °C for 30 s. At the end, PCR was run at 72 °C for 3 min for filling gaps and PCR products were analyzed subsequently using agarose gels.

2.2. Experimental stroke

The experiments have been performed following the 3R principles and ARRIVE guidelines. Induction of transient focal cerebral ischemia was approved by the Ethical Committee for Animal Research of Landesdirektion Sachsen, Germany, license number TVV 13/18. Seven days before experimental stroke, mice were transferred to the Animal Care Facility of the Medical Faculty, Leipzig University, and trained to be fed from a syringe. Transient focal cerebral ischemia in 4 months old male mice of different genotypes was performed by the filament-based model as originally described by Longa et al. (1989), with some minor adaptions. Briefly, under anaesthesia (Fentanyl, 0.05 mg/kg; Midazolam, 5 mg/kg; Medetomidin 0.5 mg/kg), a standardized filament (Doccol; Sharon, Massachusetts) was introduced into the right carotid artery and moved forward to the origin of the middle cerebral artery, and kept in place for 30 min. This procedure resulted in focal ischemia typically involving subcortical regions of the middle cerebral artery territory and, at least in part, an involvement of neocortical areas. Pain management included local anaesthesia at the medial site of the neck and the use of lidocaine (Licain; DeltaSelect, Dreieich, Germany).

After observation periods of 24 h and 72 h, mice were sacrificed by CO_2 inhalation and the brain tissue was prepared for immunohistochemical or biochemical analyses. Together, 58 WT mice and 32 DPP4 KO mice were subjected to ischemia to finally reach a group size of $N = 6$ each for biochemical and histological analyses at 24 h and 72 h after induction of ischemia. The group sizes of $N = 6$ each were based on *a priori* sample size calculations and previous experiments. Additionally, 12 WT and 12 DPP4 KO mice without ischemia served as controls for biochemical and histological analyses ($N = 6$ each). These non-ischemic animals are indicated as "control" of WT and KO origin in the respective figures.

2.3. Evaluation of functional outcome

The investigators were blind to the group allocation during the experiment and when scoring the functional outcome. The Menzies score (Menzies et al., 1992) is a clinical score to evaluate neurobehavioral deficits without relevant manipulation. Thereby, the degree of motoric deficits is recorded as follows: 0 = "no apparent deficits", 1 = „contralateral forelimb flexion", 2 = "decreased grip of the contralateral forelimb while tail pulled", 3 = „spontaneous movement in all

directions, contralateral circling only if pulled by tail“, 4 = „spontaneous contralateral circling“. Animals were scored every 24 h after reperfusion. At the same time points, animal weight was taken. In case of loss of more than 20 % of initial body weight, the animals had to be excluded from further study procedures, and were sacrificed.

2.4. Overall physical condition

As an additional outcome, the “overall physical condition” was calculated. This measure was based on Menzies score, but also included additional behavioural and mobility aspects, body weight, general appearance, and thus representing an estimate of the animals' well-being. Each parameter was scored from 0 to 3, with 3 being the worst. Score 0 included active and interested behavior, smooth, shiny coat, a weight loss of less than 5 %, and a Menzies score of 0–2. Score 1 resulted from decreased reaction and movement, dull coat, and soiled eye corners, a weight loss of less than 13 %, and a Menzies score of 3. Score 2 included chewing posture and arched back, strained breathing, stuck body openings, and shaggy coat, a weight loss of less than 20 %, and a Menzies score of 4. Score 3 in any of the parameters examined was also the termination criterion and included no response, apathy, and no locomotion in behavior and mobility. In appearance, score 3 was achieved when the animal had closed eyes, completely tousled fur and was cool.

2.5. Mouse blood and brain tissue preparation

After sacrifice, a small volume (about 0.5 ml) of blood was collected by cardiac puncture, transferred to heparin-coated vials and centrifuged immediately at 7000 × g for 10 min at 4 °C. Plasma was carefully removed from the cell pellet and stored at −80 °C.

For histological analyses, mice were transcardially perfused with 0.9 % saline followed by perfusion with 4 % paraformaldehyde in phosphate buffer (0.1 M, pH 7.4). The brains were removed from the skull and post-fixed by immersion in the same fixative overnight at 4 °C. After cryoprotection in 30 % sucrose in 0.1 M phosphate buffer for three days, 30 µm thick coronal sections were cut on a sliding microtome and collected in phosphate buffer supplemented with 0.025 % sodium azide for storage.

For biochemical analyses, mice were transcardially perfused with 0.9 % saline, the brains were removed from the skull, the cerebellum was cut off and the cerebrum was dissected into the right (ischemic) and left (control) hemispheres, frozen on dry ice and stored at −80 °C.

2.6. Calculation of infarct volumes

The infarct volume was determined by using every 9th coronal brain section for immunohistochemical NeuN+HuC/D labellings of neurons and subsequent calculation of the infarct area, which was integrated over the rostro-caudal infarct area extension. Details on respective image analyses are given below.

2.7. Immunohistochemistry

The primary antibodies against DPP4, neuronal, glial and inflammatory marker proteins used in this study are listed in Table 1. The specificity of the goat antiserum against DPP4 was verified in brain tissue of DPP4 KO mice by the absence of the typical, microvessel-associated DPP4 immunoreactivity present WT mouse brain (see Results). The goat anti-CCL2 antibody used did not generate immunohistochemical labelling in non-ischemic WT and DPP4 KO mouse brain but detected diffuse and granular extracellular and cellular labelling in ischemic WT and DPP4 KO mouse brain tissue (see Results). In ischemic brain tissue of CCL2 KO mice, no CCL2 immunosignals were detected (not shown).

Table 1
Cocktails of primary and corresponding biotinylated (Bio-) or carbocyanin-labelled (Cy) secondary antibodies used for single and multi-immunofluorescent labellings in mouse brain.

Primary antibody	Dilution	Company	Cat. #	Secondary antibody
NeuN	1:1000	Millipore	MAB377	Cy5 donkey anti-mouse
HuC/D	1:1000	Invitrogen	A-21271	Cy5 donkey anti-mouse
NFL	1:200	Synaptic Systems	171002	Cy2 donkey anti-rabbit
DPP4	1:50	R&D	AF954	Cy3 donkey anti-goat
CCL2	1:100	R&D	AF479	Cy3 donkey anti-goat
CD68	1:100	Biorad	MCA1957	Cy2 donkey anti-rat
TMEM119	1:100	abcam	ab209064	Cy3 donkey anti-rabbit
NeuN	1:1000	Millipore	MAB377	Cy3 donkey anti-mouse
HuC/D	1:1000	Invitrogen	A-21271	Cy3 donkey anti-mouse
Iba1	1:500	WAKO	019-19741	Cy2 donkey anti-rabbit
GFAP	1:200	Synaptic Systems	173004	Cy5 donkey anti-guinea pig
NeuN	1:1000	Millipore	MAB377	Bio donkey anti-mouse
HuC/D	1:1000	Invitrogen	A-21271	Bio donkey anti-mouse
MHC-II	1:500	Invitrogen	14-5321-82	Bio donkey anti-rat

2.7.1. Single labelling of NeuN and HuC/D in mouse brain sections

In order to detect significant neuronal populations in brain of WT and DPP4 KO mice, single labelling immunohistochemistry with cocktails of mouse antibodies against NeuN and against HuC/D was performed on free-floating coronal brain sections. Brain sections were washed in 0.1 M phosphate buffer (pH 7.4) for 5 min and endogenous peroxidases were inactivated by treating brain slices with 60 % methanol containing 0.3 % H_2O_2 for 60 min followed by three washing steps with Tris buffered-saline (TBS, 0.1 M, pH 7.4) for 5 min each. After masking unspecific binding sites with blocking solution (3 % donkey anti-mouse IgG Fab fragment, 2 % normal donkey serum in TBS containing 0.3 % Triton X-100) for 60 min, sections were incubated in 5 % normal donkey serum in TBS containing 0.1 % Triton-X-100 with the primary antibodies as indicated in Table 1 for 24 h at 4 °C. Brain sections were then washed three times in TBS for 5 min each before being incubated with biotinylated secondary donkey anti-mouse antibodies (Dianova; 1:1000) in TBS containing 2 % bovine serum albumin (BSA) for 60 min. After three washing steps in TBS for 5 min each, slices were incubated with ExtrAvidin peroxidase (Sigma; 1:2000) in TBS/2 % BSA followed by washing steps and pre-incubation in Tris buffer (0.05 M, pH 7.6) for 5 min. Finally, visualization of peroxidase binding was performed by incubation with 4 mg 3,3′-diaminobenzidine (DAB) and 2.5 µl 30 % H_2O_2 per 5 ml Tris buffer. After washing, sections were mounted onto glass slides and cover slipped.

2.7.2. Double and triple immunofluorescent labellings in mouse brain

In order to reveal the expression of DPP4, CCL2 and affected immune cells in ischemic mouse brain areas, cocktails of primary antibodies from different species were used as specified in Table 1. Brain sections were incubated with cocktails of primary antibodies for 24 h at 4 °C. Sections were then washed three times with TBS followed by incubation with cocktails of Cy2-, Cy3- or Cy5-conjugated donkey anti-mouse, −rabbit, −guinea pig, −rat or -goat, respectively, antisera (1:500 each; Dianova) in TBS containing 2 % BSA for 60 min at room temperature. After washing, sections were mounted onto glass slides and cover slipped.

Switching the fluorescent labels of the secondary antibodies

generated similar results as when following the procedure outlined above (not shown). For all single, double and triple immunohistochemical labellings in brain sections described above, control experiments in the absence of primary antibodies were carried out. In each case, this resulted in unstained brain sections (not shown). In addition, the specificity of the primary antibodies against DPP4 and CCL2 was validated in non-ischemic and ischemic brain tissue of WT and the respective KO genotype.

2.8. Microscopy

2.8.1. Light microscopy

Mouse brain tissue sections immunohistochemically stained with DAB or DAB-Ni for NeuN+HuC/D and for MHC-II expression were examined with an Axio-Scan.Z1 slide scanner connected with a Colibri.7 light source and a Hitachi HV-F202SCL camera (Zeiss; Göttingen, Germany). High resolution images of brain sections were taken using a 20× objective lens with 0.8 numerical aperture (Zeiss). Images were digitized using the ZEN blue 2.6 software.

2.8.2. Fluorescence microscopy

Brain tissue sections of WT and KO mice immunochemically stained with Carbocyanine-labelled secondary antibodies were examined with an AxioScan.Z1 microscope (Zeiss; Göttingen, Germany) equipped with a Colibri 7 light source including 6 LEDs covering the light spectrum from 385 to 735 nm to generate seven fluorescence excitation lines for the samples to be analyzed. All LEDs besides the green/yellow line (combined 555/590 nm filter changer) come with individual excitation filters. Emission filters selected were: for Cy2 at 524 nm, for Cy3 at 595 nm and for Cy5 at 676 nm. Pictures were taken using the Axiocam 506 and a Plan-Apochromat objective (20×/0.8) and exposure times of 15 ms for Cy2, 20 ms for Cy3 and 30 ms for Cy5. Images were digitized using the ZEN blue 2.6 software.

2.8.3. Image analysis

Images were analyzed using the ZEN 3.4 Blue Edition (Zeiss; Göttingen, Germany). Additionally, the deep learning toolkits ZEN Module Intellesis and arivis Cloud (formerly named Apeer) enabling automated threshold-based segmentation were used to quantify immunofluorescent stainings. Employing machine learning protocols, errors and influences of user bias were avoided. For single neuronal staining the area lacking NeuN and HuC/D immunoreactivity was determined manually and calculated by the ZEN software. For DPP4 quantification, segmentation for vessel-like structures was performed and the signal intensity was measured, since the stained area was not affected obviously. For Iba1 staining, the training was aimed to recognize the number of morphological reactive microglia (enlarged cell body, less branches), but not surveying microglia (small cell body, long branches). The final analysis revealed the number of these cells. MHC-II positive cells were analyzed manually in the brain parenchyma since trainable segmentation would always include the MHC-II positive cells in vessels which we wanted to exclude due to the unknown place of destination. For quantification of CCL2, the amount of signals regardless of the signal size was determined. For GFAP, CD68 and TMEM119, the area covered by a positive signal was analyzed because individual cells could not be discriminated. The NFL immunosignals were also analyzed by total area due to the mixed intra- and diffuse extracellular staining.

2.8.4. Quantification of chemokines in brain tissue and plasma

2.8.4.1. Cerebrum preparation. In order to prepare mouse cerebrum for Bio-Plex analysis, the left and right cerebrum of the ischemic group and right cerebrum of non-ischemic control mice were homogenized in T-Per buffer (Tissue Protein Extraction Reagent, Thermo Fisher Scientific; Darmstadt, Germany) at a concentration of 333 mg/ml with Protease Inhibitor Cocktail Tablets (Merck; Darmstadt, Germany) by using a Precellys homogenizer (VWR; Dresden, Germany). The homogenate was centrifuged for 15 min at 10,000 ×g at 4 °C, kept on ice for transferring to 1.5 ml reaction tubes and centrifuged again for 30 min at 25,000 ×g at 4 °C. The soluble supernatant was collected, aliquoted and stored at −80 °C until use.

2.8.4.2. BCA protein assay. The BCA assay (Pierce, Thermo Fisher Scientific; Darmstadt, Germany) was performed according manufacturer's protocol. Cerebrum samples were diluted 1:50 in T-Per buffer. Albumin standard working range corresponded to 20–2000 µg/ml ($n = 2$). Absorption was measured at 562 nm (Tecan Sunrise; Männedorf, Switzerland).

2.8.4.3. Bio-Plex analysis. For multiplex analysis of chemokines in plasma and cerebrum, an individually prepared 8-Plex (Bio-Rad; Feldkirchen, Germany) was used. The following cytokines were included: fractalkine/CX3CL1, IL-1β, IL-6, MCP-1/CCL2, MCP-5/CCL12, RANTES/CCL5, TARC/CCL17 and TNF-α. At the beginning, all desired cytokine beads were combined and 50 µl of the suspension was added per well to a 96-well plate. After washing twice, the samples (plasma diluted 1:4 in Sample Diluent or brain tissue homogenate diluted 1:10 in Sample Diluent containing 0.5 % BSA), standards and blanks were transferred to the appropriate wells. Further steps of the implementation were made according to the manufacturer's instructions.

2.8.4.4. Statistical analysis. To compare differences between the ischemic hemisphere and the non-ischemic control hemisphere of the same brain, we used Wilcoxon Signed Rank test. To compare differences between WT and the respective KO mice, Mann-Whitney Rank Sum test was used. For calculations and visualization GraphPad Prism 10.0 (GraphPad Software, Boston, USA) was used. Differences between groups were considered statistically significant for p values <0.05. Statistical differences of survival rates of WT and DPP4 KO mice were calculated by Log-Rank (Mantal-Cox) test.

3. Results

3.1. Characteristics of focal cerebral ischemia in WT and DPP4 KO mice

The health status of mice after experiencing MCAO was tightly monitored. This included daily recordings of the Menzies score, behavior and mobility, general appearance and body weight. While no mice had to be sacrificed based on the pre-determined termination criteria on weight loss or signs of physical deterioration, we observed a stable Menzies score and an increasing impairment in the overall physical condition over time for both genotypes (Fig. 1A). Strikingly, DPP4 KO mice displayed a much higher survival rate of 72 % after MCAO compared to the WT animals (45 %) (Fig. 1A). On the other hand, body weight loss was more pronounced in the DPP4 KO (16 %) group after MCAO than in the WT cohort (7 %) (Fig. 1A).

To quantify the infarct size at 24 h and 72 h after ischemia, independent analyses using immunohistochemistry for NeuN+HuC/D and for Neurofilament L were performed. While NeuN+HuC/D immunosignals were reduced in the infarct area, the signals for Neurofilament L were increased in the affected brain regions (Fig. 1B, C). Neither the infarct volume calculated from NeuN+HuC/D labellings along the rostro-caudal infarct extension nor the infarct area calculated from Neurofilament L immunohistochemistry revealed differences between the genotypes or time points analyzed (Fig. 1C).

Next, we analyzed the expression of DPP4 in control mice without ischemia and on the ipsi- and contralateral brain hemisphere of mice after ischemia for 24 h and 72 h. Typically, DPP4 immunoreactivity appeared in the vasculature and was more pronounced in the ischemic animals than in control animals of the WT genotype (Fig. 2A). In DPP4

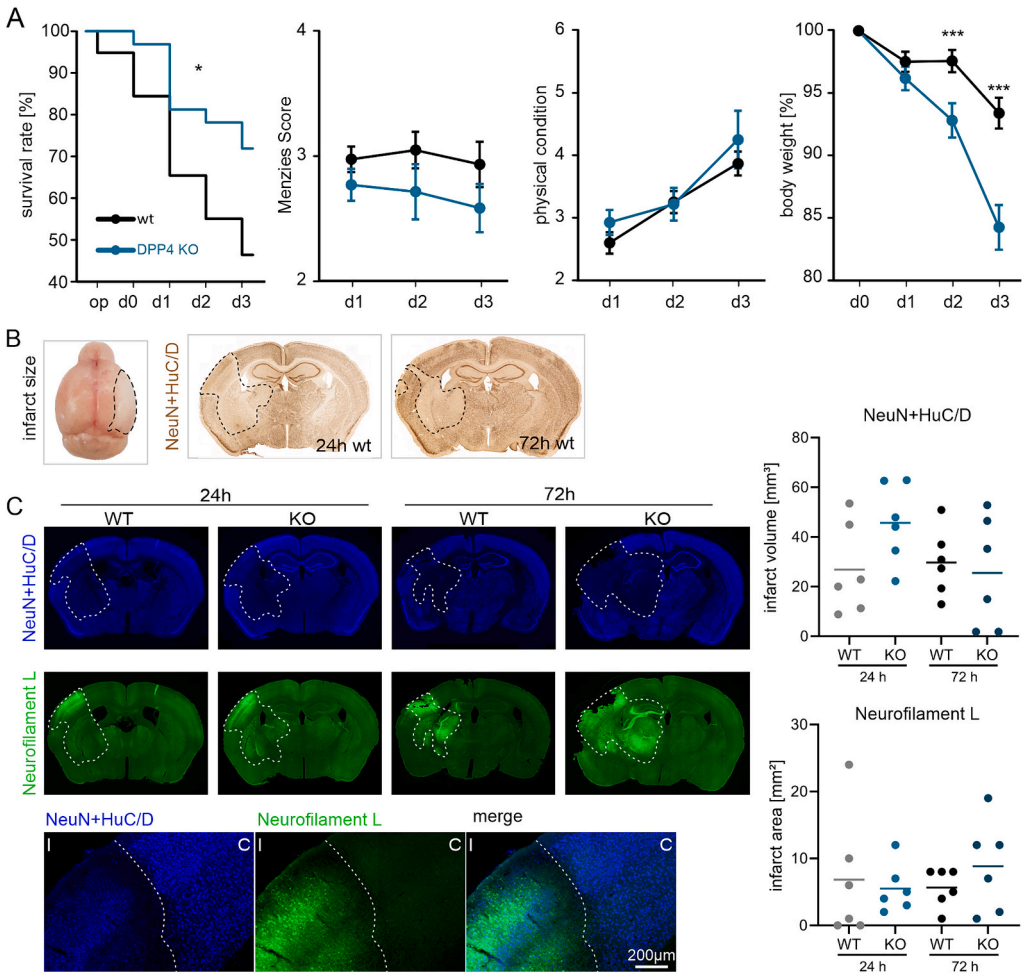

Fig. 1. Characterization of focal cerebral ischemia in DPP4 knock-out mice. Mice of wild type (WT) and DPP4 knock-out (KO) genotypes were subjected to transient focal cerebral ischemia for 30 min, followed by 24- and 72-h observation periods. (A) Survival rate, Menzies score, overall physical condition and body weight for WT and DPP4 KO genotypes. Only 45 % (WT) and 72 % (DPP4 KO) of the animals subjected to the operation procedure survived for 72 h. The subsequent drop out from 58 WT mice and 32 DPP4 KO mice initially enrolled were (WT/DPP4 KO): (i) during surgery: 3/0, (ii) day 0: 6/1, (iii) day 1: 11/5, (iv) day 2: 6/1 and (v) day 3: 5/2. For both genotypes, a constant mean Menzies Score of 2.5 to 3 was determined at all time points. In contrast, the overall physical condition steadily declined (higher scores indicating worse condition) during the 72-h post-surgery period, which was also characterized by a weight loss ranging between 7 % in WT mice and 16 % in DPP4 KO mice. For neurological score, overall physical condition and body weight assessment, all mice alive at the respective time points were considered. Error bars represent SEM values. (B) Macroscopic delineation of the infarct area and immunohistochemical NeuN+HuC/D images in histological brain sections from experimental animals at 24 and 72 h after onset of ischemia. The dashed lines indicate the infarct area identified by diminished NeuN+HuC/D labelling. (C) Immunohistochemical double labelling of NeuN+HuC/D (blue) and NeuN (green) in coronal mouse brain sections of ischemic animals as indicated. Note the complementary loss of NeuN+HuC/D and induction of NFL immunoreactivity in the ischemic area (I) compared to control tissue (C). The infarct volume was calculated from NeuN+HuC/D-labelled serial brain slices for all animals of both genotypes and displayed mean values between 26 mm^3 (KO, 72 h) and 45 mm^3 (DPP4 KO, 24 h). (C) As a complementary measure of infarct size, increased immunosignals for NFL in the ischemic area were quantified in serial sections. Here, constant ischemic areas for both genotypes and time points between 5.5 and 8.8 mm^2 were detected. (For interpretation of the references to colour in this figure legend, the reader is referred to the web version of this article.)

KO mouse brain tissue, this labelling was absent, demonstrating the specificity of the DPP4 antibody and the correct genotyping of the mice (Fig. 2A). Immunofluorescent double labelling of DPP4 with NeuN+HuC/D allowed for the visualization of DPP4 immunoreactivity at the infarct border zone (Fig. 2B). We noticed a lower background in the ischemic tissue after DPP4 immunofluorescent labelling, which precluded using the overall immunofluorescence signal in the ischemic area for quantification of DPP4. Instead, a trainable segmentation protocol was established to quantify the DPP4 signal intensity selectively for the vascular structures (Fig. 2C). The subsequent batch analysis demonstrated (i) the absence of DPP4 immunosignals in DPP4 KO mouse brain tissue regardless of duration of MCAO, (ii) an increasing DPP4 immunoreactivity from 24 h to 72 h of ischemia at the control side of ischemic WT mice and compared to control mice without ischemia and (iii) lower DPP4 immunoreactivity at the ischemic side than at the control side of WT mice at both time points (Fig. 2C).

3.2. Cellular and molecular responses to ischemia in WT and DPP4 KO mice

CCL2, which is known to be robustly induced after ischemia, was then quantified in brains WT and DPP4 KO mice at 24 h and 72 h after MCAO. Immunohistochemical labellings revealed the presence of CCL2 as granular, most likely extracellular, immunosignals in the infarct area identified by reduced NeuN+HuC/D immunoreactivity but also expanding into the unaffected brain tissue (Fig. 3A). The quantification of CCL2 immunoreactivity revealed a robust and time-dependent increase in ischemic WT animals which was not observed in ischemic DPP4 KO animals (Fig. 3B). CCL2 was found to be associated with cerebral blood vessels and with different cell types including microglia,

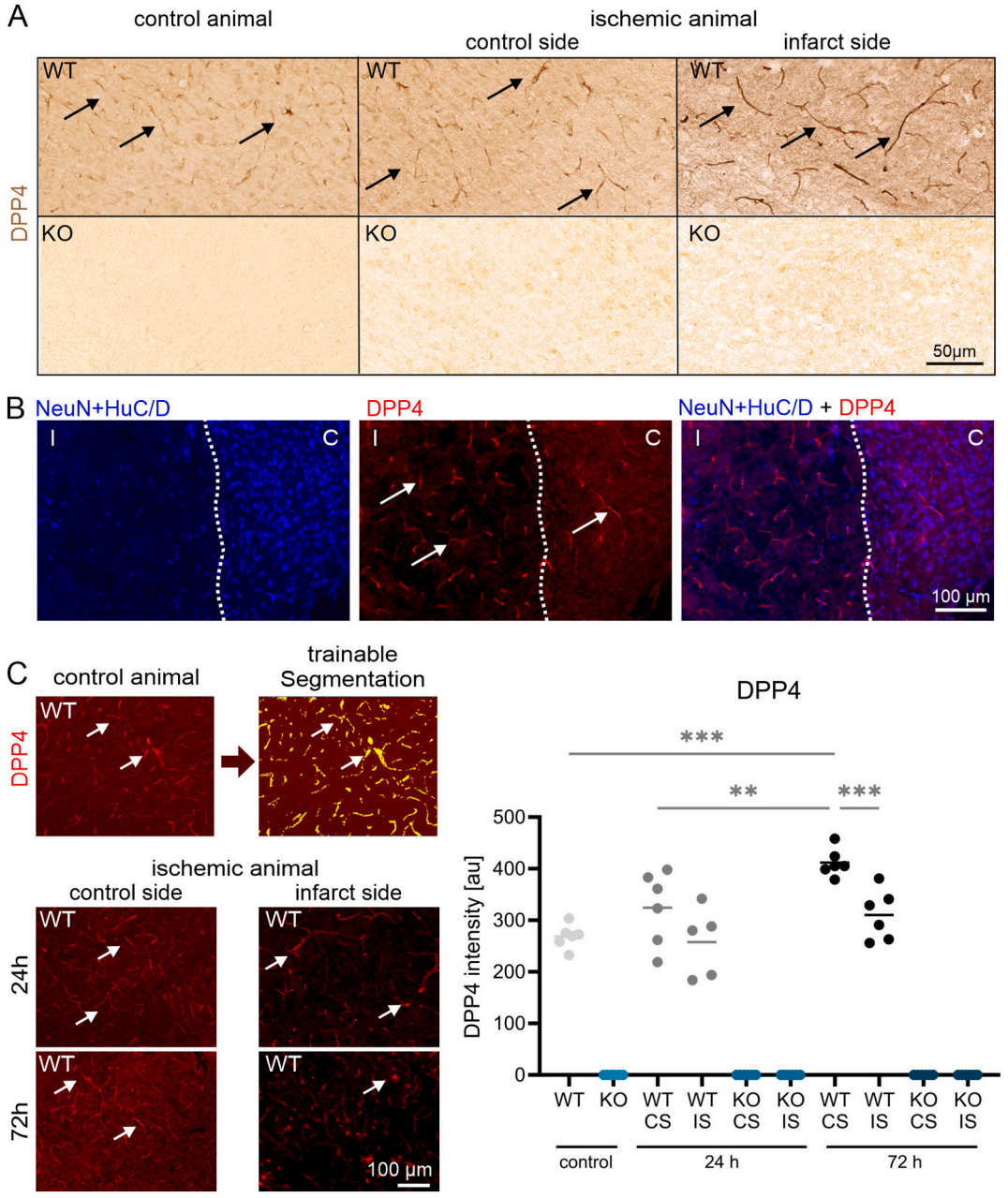

Fig. 2. Expression of DPP4 in ischemic brain areas. (A) Immunohistochemical labellings for DPP4 in wild type (WT, top) and in DPP4 KO (KO, bottom) mouse brain in control animals without ischemia and at the control side and infarct side 72 h after ischemia. Note the labelling of vasculature in WT mouse brain and the absence of DPP4 immunoreactivity in the DPP4 KO brain sections. (B) Visualization of DPP4 immunoreactivity (arrows) at the infarct border zone identified by loss of NeuN+HuC/D labelling in the ischemic area (I). (C) Depiction of the trainable segmentation performed on DPP4-labelled brain slices with ZEN Intellesis and typical examples of DPP4 immunoreactivity at the control and ischemic hemisphere of ischemic WT animals at 24 h and 72 h after ischemia as indicated. The quantification of DPP4 immunoreactivity revealed lower DPP4 levels at the ischemic hemisphere (IS) compared to the control hemisphere (CS). "Control" refers to non-ischemic animals of WT or DPP4 KO origin as indicated. ** $p < 0.01$; *** $p < 0.001$; statistically significant.

neurons and astrocytes (not shown).

Since CCL2 is known to mediate recruitment of immune cells to the site of tissue damage, we next analyzed the abundance of activated Iba1-positive microglia cells and GFAP-immunoreactive astrocytes in the brains of WT and DPP4 KO mice after ischemia. Triple immunofluorescent labellings of microglia and astrocytes with the neuronal markers NeuN+HuC/D revealed a specific activation of microglia in the ischemic brain tissue and of astrocytes at the peri-infarct area, forming a border between affected and unaffected brain tissue (Fig. 4A). The quantification of the respective immunosignals demonstrated a robust increase in activated microglia at 72 h after ischemia in WT mouse brain, which was significantly lower in DPP4 KO mouse brain (Fig. 4B). This finding is in line with the observed lower levels of CCL2 in DPP4 KO mouse brain at this post-ischemic time point, which might be one factor contributing to diminished microglia activation. The GFAP immunoreactivity, on the other hand, was already increased at 24 h after ischemia in both genotypes and maintained at this level until 72 h after ischemia (Fig. 4C).

It is known that specific subsets of microglia display differential responses to insults of the brain tissue. We, therefore, analyzed abundance of CD68- and of TMEM119-immunoreactive microglia and of infiltrated MHC-II-positive immune cells in brains of WT and DPP4 KO mice at 24 h and 72 h after ischemia. The CD68 immunoreactivity did not differ

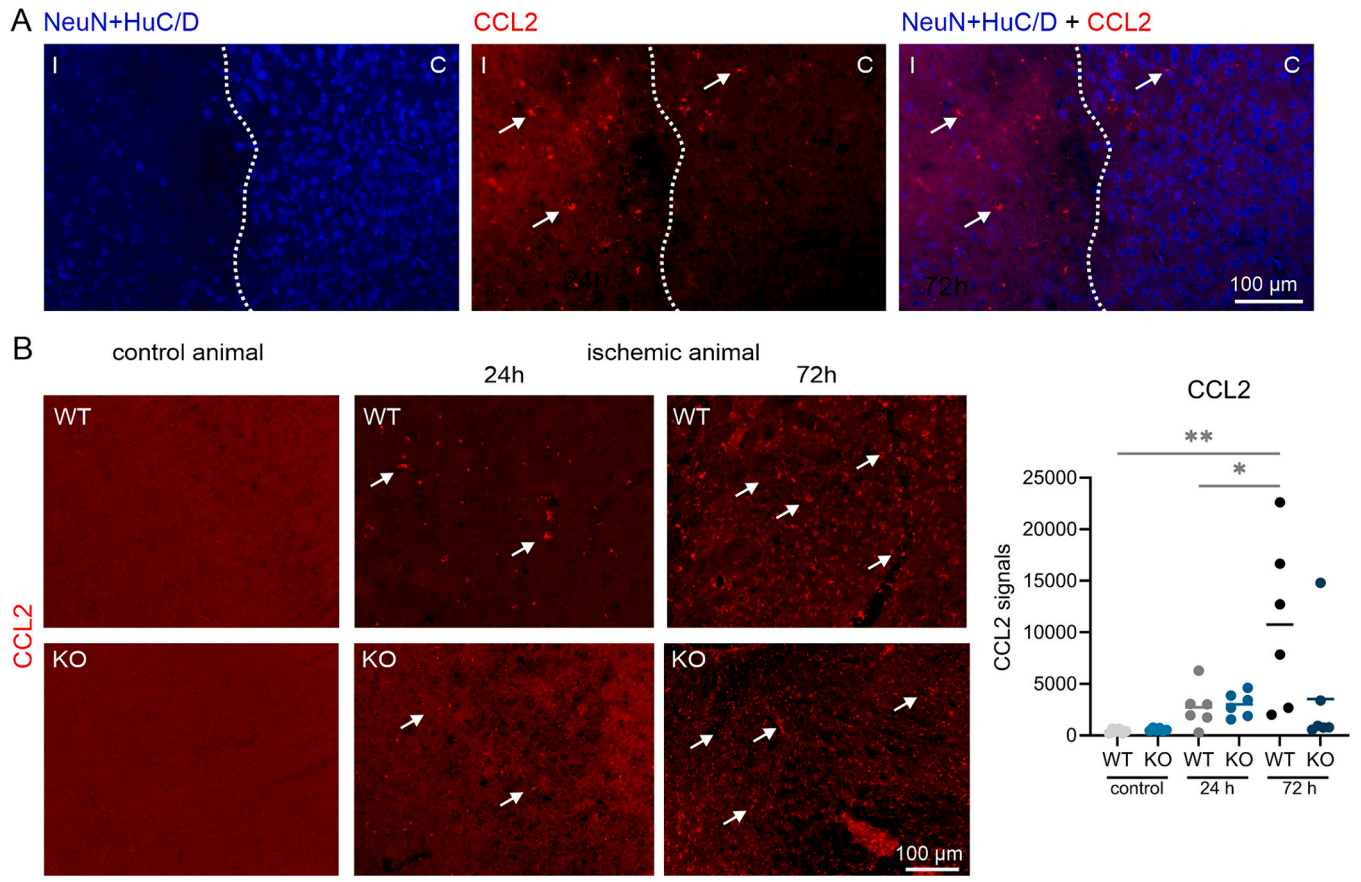

Fig. 3. Quantification of CCL2 expression and co-localization to the ischemic area. (A) Double immunohistochemical labelling of CCL2 (red) in combination with NeuN+HuC/D (blue) in a wild type (WT) mouse brain 24 h after ischemia. Note the strong CCL2 immunoreactivity in the infarct area (I) and the spreading of CCL2 immunosignals into the border zone (arrows). (B) CCL2 immunoreactivity was absent in the non-ischemic WT and DPP4 KO control mouse brain and appeared for the most part as extracellular spots that gradually increased from 24 h to 72 h of ischemia. Quantification of CCL2 immunosignals demonstrating steadily increased CCL2 in WT mouse brain at 24 and 72 h. Note that the time-dependent increase in CCL2 signals was not present in ischemic DPP4 KO mouse brain tissue. "Control" refers to non-ischemic animals of WT or DPP4 KO origin as indicated. * $p < 0.05$; ** $p < 0.01$; statistically significant effects of ischemia. (For interpretation of the references to colour in this figure legend, the reader is referred to the web version of this article.)

between non-ischemic control mice of WT and DPP4 KO (Fig. 5A). Under ischemic conditions, there were no differences in CD68 immunosignals between genotypes and compared to non-ischemic conditions (Fig. 5A). On the other hand, there was a marked and post-ischemia time-dependent reduction in TMEM119 immunoreactivity in both genotypes compared to their non-ischemic control mice (Fig. 5B). In addition, we observed higher numbers of parenchymal MHC-II-positive immune cells in both, WT and DPP4 KO mouse brain (Fig. 5C).

To reveal the effects of DPP4 KO on the expression of a panel of chemokines and cytokines under ischemic conditions, CCL2, CCL5 CCL12, CX3CL1, IL-6, IL-1β, CCL17 and TNF-α concentrations were quantified by multiplex analysis in brain and plasma of WT and DPP4 KO mice (Fig. 6). Most cytokines analyzed displayed increased concentrations under ischemic conditions in both brain and plasma of WT and DPP4 KO mice, which reached statistical significance for CCL5, CCL12 and CCL17. Interestingly, when effects of the DPP4 KO were observed, the respective chemokine concentrations were lower than in WT mice. This holds true for CCL5 in plasma at 72 h after ischemia, for CCL12 at 24 h after ischemia and for CCL17 in brain tissue at 72 h of ischemia (Fig. 6) and is indicative of a general anti-inflammatory effect of DPP4 ablation.

4. Discussion

The aim of the present study was to investigate the effects of DPP4 deficiency on the molecular, cellular, and functional outcome of stroke. In particular, we hypothesized that diminished DPP4 enzymatic activity would affect molecular and cellular aspects of neuroinflammation. The applied experimental models included DPP4 KO mice and the filament model of transient MCAO, which have several advantages and limitations. On the one hand, genetic ablation of DPP4 results in a complete and specific inhibition of its enzymatic activity, which cannot be achieved by pharmacologic DPP4 inhibition. On the other hand, DPP4 KO affects both, its enzymatic and non-enzymatic functions which cannot be distinguished in this setup and thus represents a limitation of the study. Moreover, because of the constitutive DPP4 KO, the potential stroke treatment effect persists from birth onwards and is not initiated in a meaningful therapeutic window after the onset of stroke. There are also limitations regarding the identification of microglial subtypes detected by Iba-1, CD68 and TMEM119 antibodies. Of note, these cell surface markers are not specific for microglial cells but might be expressed, depending on the experimental setup, also by monocytes and/or infiltrating macrophages (Spiteri et al., 2020; Lier et al., 2021; Vankriekelsvenne et al., 2022). However, the low number of MHC-II-positive infiltrating macrophages detected here in brain parenchyma indicates that most Iba-1, CD68 and TMEM119-positive cells are indeed microglia. The stroke model employed in the present study is been used in numerous experimental setups and is widely accepted in the field of preclinical stroke research, especially because of its reproducibility concerning infarct location and size (Durukan and Tatlisumak, 2007). Some earlier studies applied laser Doppler cerebral blood flow measurement over the MCA territory to confirm blood flow reduction. In the

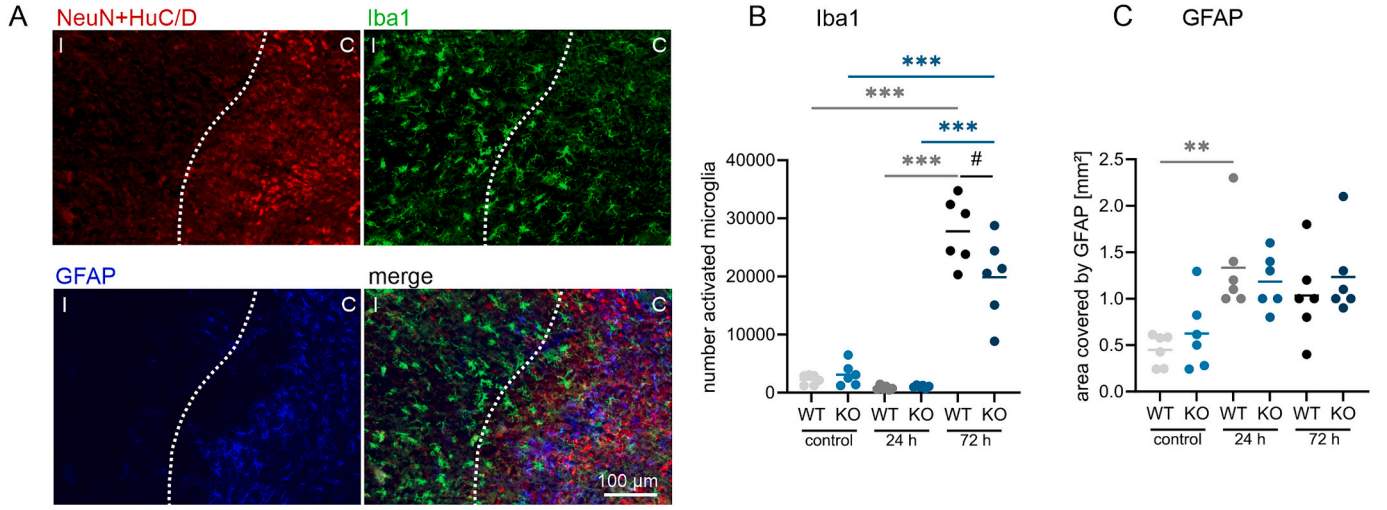

Fig. 4. Activation of microglia and astrocytes in ischemic brain regions. (A) Triple immunofluorescent labellings of the microglial marker Iba1 (green) and the astrocyte marker GFAP (blue) in combination with NeuN+HuC/D (red) to identify the infarct area (I) at 24 h after ischemia. Note the activation of microglia in the infarct region and extending into the infarct border zone, whereas GFAP immunoreactivity is indicative of an astrocytic barrier formation in the non-ischemic tissue. (B) The quantification of activated Iba1-positive microglia demonstrates the delayed activation only at 72 h after ischemia, which is less pronounced in DPP4 KO mice. "Control" refers to non-ischemic animals of WT or DPP4 KO origin as indicated. (C) The quantification of activated GFAP-positive astrocytes demonstrates their instant activation at 24 h after ischemia, which persists at 72 h of ischemia. There are no differences in GFAP immunoreactivity between WT and DPP4 KO mice. ** $p < 0.01$; *** $p < 0.001$; statistically significant effects of ischemia, # $p < 0.05$; statistically significant effects between WT and DPP4 KO. (For interpretation of the references to colour in this figure legend, the reader is referred to the web version of this article.)

present study, we decided to omit this blood flow measurement as it would have been extended the anaesthesia period markedly. Instead, we used the clinical Menzies score as a non-invasive control for brain infarction. In addition, general limitations need to be considered regarding the transferability from finding in the preclinical field into clinical routine (Young et al., 2007).

We observed a striking and statistically significant improvement of the survival rate after stroke in DPP4 KO mice compared WT mice. This is in line with earlier observations using DPP4 inhibitors in mouse and rat stroke models demonstrating effects of DPP4 inhibition on (i) stroke prevention, (ii) acute neuroprotection, and (iii) post-stroke recovery (for reviews see Darsalia et al., 2015, 2018, 2019). However, the functional Menzies score was not improved in DPP4 KO mice. In addition, DPP4 KO mice lost significantly more body weight after experimental stroke than WT mice. The cause of death and reasons for improved survival of DPP4 KO mice after ischemia, in the absence of functional improvements and in the presence of weight loss, remain uncertain. Generally, death rates depend on a large number of factors, including, for instance, the mouse strain, the animal's age and condition before ischemia, the specific procedure to induce ischemia (including use of anesthetics, temperature control, *etc.*), the duration of ischemia, the post-ischemic care conditions, and the planned observation period. Survival rates of C57BL/6 mice following MCAO ischemia had been addressed in a few former studies, indicating a complex interplay between genetic predisposition, vascular anatomy, and inflammatory responses. Thus, based on the anti-inflammatory effects observed, it might be speculated that these contribute to better survival rates. A follow-up study with longer post-ischemic survival times might reveal whether death is indeed prevented or only delayed. DPP4 inhibitors are reported to stabilize or even reduce body weight in diabetes therapy (Esposito et al., 2019) and to robustly reduce body weight in a mouse obesity model (Chae et al., 2015). However, in our model WT and DPP4 KO mice started with an identical body weight and the pronounced weight loss in DPP4 KO mice occurred after MCAO. This might be critical in experiments designed to evaluate long-term survival after stroke.

There were no differences between WT and DPP4 KO mice in cross-sectional infarct area or the infarct volume calculated along the rostro-caudal brain extension. This contrasts previous experiments, where the application of DPP4 inhibitors in mouse stroke models resulted in less neuronal loss and thus a smaller infarct volume (Darsalia et al., 2013; Chiazza et al., 2018). This indicates a detrimental role of enzymatically active DPP4 in stroke that can be addressed by DPP4 inhibitors. Another recent study measured DPP4 activity in venous blood samples at hospital admission and found significantly higher DPP4 activity in stroke patients with a larger infarct volume (Baerts et al., 2017). The precise mechanism behind the possibly neuroprotective feature of DPP4 inhibition has not yet been sufficiently clarified, as its substrates are involved in numerous physiological processes ranging from neuroendocrinology over metabolism and immune response to the cardiovascular system (Klemann et al., 2016). One of the substrates cleaved by DPP4, GLP-1, has known anti-inflammatory properties (Steven et al., 2019). Large clinical trials, like LEADER and SUSTAIN-6 focusing on medication with GLP-1 analogues have proven its beneficial effects on cardiovascular health and even resulted in a significant lower rate of nonfatal stroke (Marso et al., 2016a, 2016b). The lack of effect of DPP4 KO on infarct size in our study compared to the pharmacological studies reported above might be due to different experimental setups: genetic *versus* pharmacologic DPP4 inhibition, variations in stroke protocols including survival times, genetic background of the mice and sample size.

We considered it crucial to monitor the expression of DPP4 itself in WT mice under ischemic and non-ischemic conditions. First, this allowed to detect alterations of DPP4 expression after ischemia. In addition, the correct genotype and the specificity of the DPP4 antibody used were validated. DPP4 immunoreactivity was found to be present in the vasculature. Surprisingly, DPP4 immunoreactivity was increased in the non-ischemic control hemisphere, but not in the ischemic hemisphere, of ischemic mice compared to non-ischemic mouse brain tissue. The reason for this effect is not known but could be based on compensatory effects in the control hemisphere.

Next, the expression of the pro-inflammatory chemokine CCL2 was monitored in brain tissue of WT and DPP4 KO mice at 24 h and 72 h after ischemia. CCL2 is known to contribute to inflammatory processes in brain, including traumatic brain injury (Gyoneva and Ransohoff, 2015), epilepsy (Arisi et al., 2015), tumors (Leung et al., 1997; Lindemann et al., 2015), Alzheimer's disease (AD) (Hartlage-Rübsamen et al., 2015;

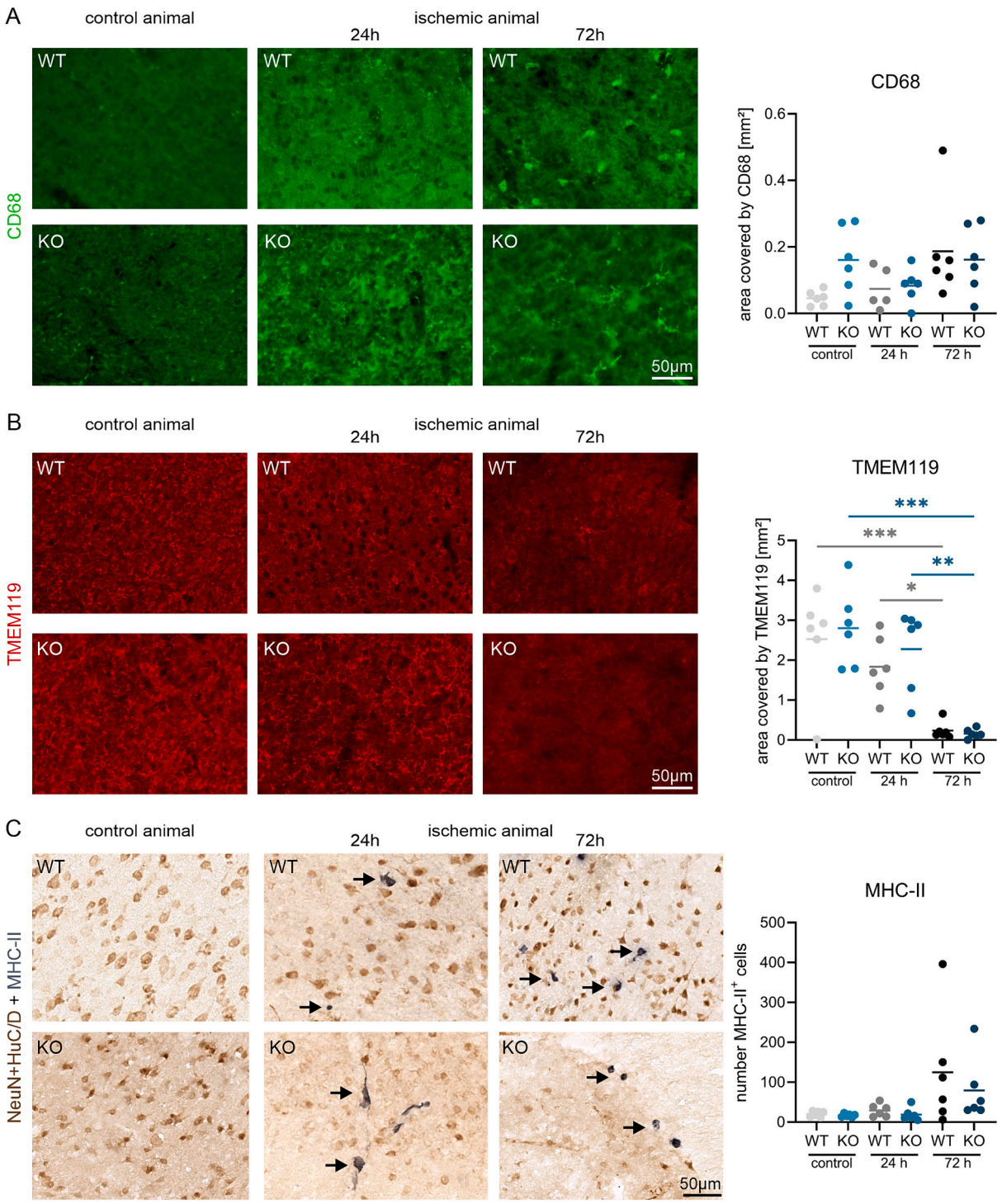

Fig. 5. Activation and recruitment of CD68-, TMEM119- and MHC-II-positive immune cells in ischemic brain regions.
(A) In non-ischemic mice ("control"), CD68-positive cells appeared to be more abundant in brain tissue of DPP4 KO mice tissue than in WT mice. In ischemic WT mouse brain, CD68 immunoreactivity steadily increases from 24 h to 72 h after ischemia. This increase is not detected in DPP4 KO mouse brain tissue. (B) TMEM119 immunoreactivity gradually decreases at 24 h and 72 h after ischemia for both genotypes, compared to non-ischemic mice of both genotypes ("control"). (C) Numbers of MHC-II^{+} cells only increased at 72 h after ischemia for both genotypes and were not detected in non-ischemic mice ("control"). * $p < 0.05$; ** $p < 0.01$; *** $p < 0.001$; statistically significant effects of ischemia.

Sokolova et al., 2009; Westin et al., 2012) and stroke (Worthmann et al., 2010; Kuriyama et al., 2009). Interestingly, in CCL2 KO mice the infarct size, levels of pro-inflammatory markers and blood-brain barrier breakdown were found to be reduced and the functional outcome was improved after focal cerebral ischemia compared to WT animals (Strecker et al., 2011, 2013; Schuette-Nuetgen et al., 2012). This would suggest that a pharmacologic reduction of biologically active CCL2 has therapeutic potential in ischemic conditions and presumably also in other brain disorders with a neuroinflammatory component. However, this assumption is challenged by recent studies demonstrating that deletion of the CCL2 receptor CCR2 contributes to increased cerebral ischemic injury (Gliem et al., 2015, 2016; Wattananit et al., 2016). We,

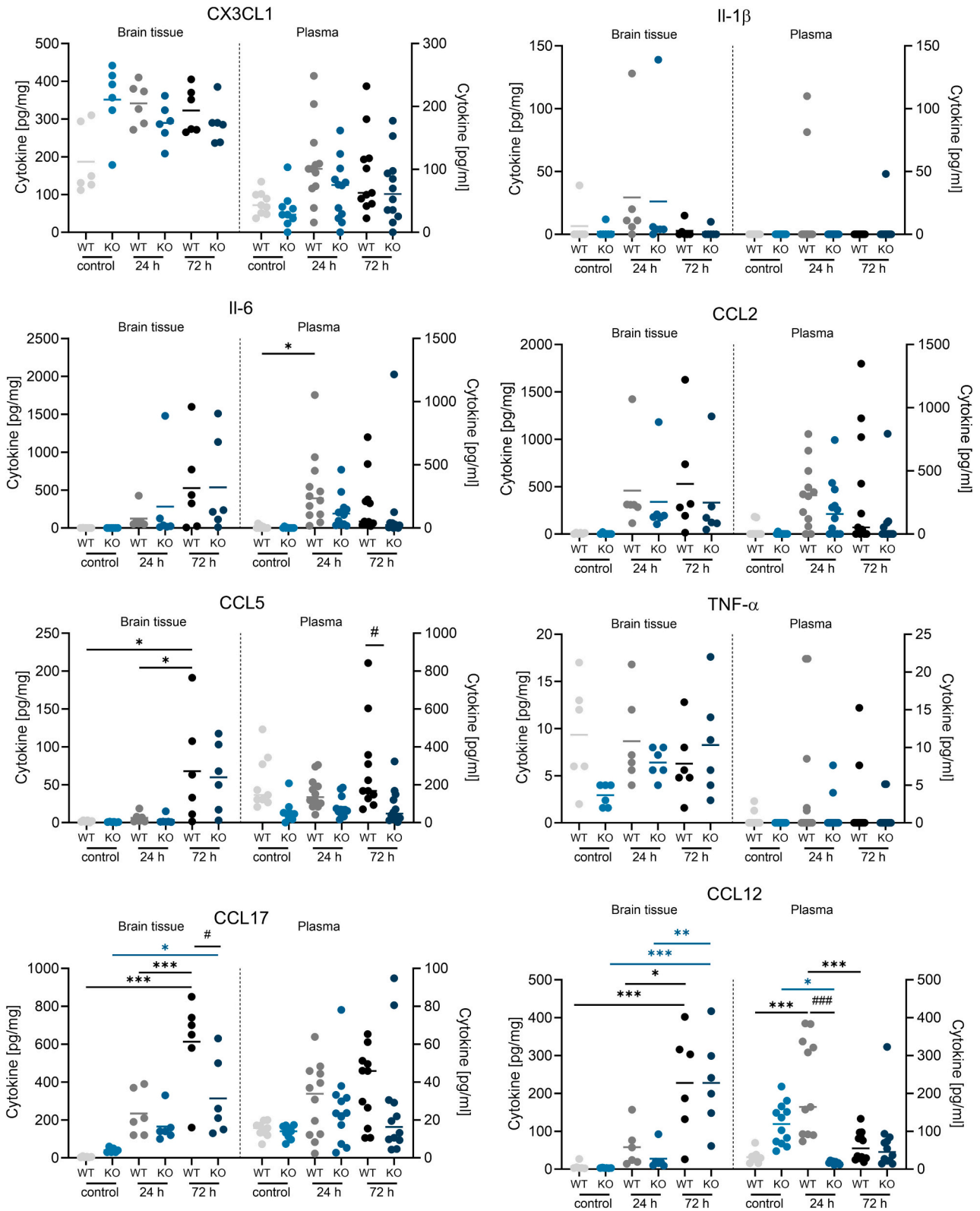

Fig. 6. Quantification of chemokines in brain tissue and plasma of mice after ischemia. The concentrations of a number of chemokines and cytokines (CCL2, CCL5, CCL12, CX3CL1, IL-6, IL-1β, CCL17 and TNF-α) were quantified by multiplex analyses in brain tissue of the ischemic hemisphere and in plasma as indicated at 24 h and 72 h after ischemia as indicated. There was a (time-dependent) increase for most of these factors after ischemia, except for IL-1β, and TNF-α. There were reductions in plasma concentrations of DPP4 KO mice for CCL5 mice at 72 h of ischemia and for CCL12 at 24 h of ischemia as well as in brain tissue of DPP4 KO mice for CCL12 at 72 h of ischemia. "Control" refers to non-ischemic animals of WT or DPP4 KO origin as indicated. * $p < 0.05$; ** $p < 0.01$; *** $p < 0.001$; statistically significant effects of ischemia; # $p < 0.05$; ### $p < 0.001$; statistically significant effects between WT and DPP4 KO.

therefore, systematically investigated the expression of CCL2 under conditions of cerebral ischemia *in vivo* in WT and DPP4 KO mice. We observed a slight increase in CCL2 immunoreactivity at 24 h of ischemia and a robust increase after 72 h of ischemia in WT brain tissue. However, in DPP4 KO brain tissue, the levels of CCL2 were not increased after ischemia and much lower than in ischemic WT mouse brain tissue. In this context, immature CCL2 has been shown to be a DPP4 substrate but the N-terminus of mature CCL2 is fully blocked by a pyroglutamate residue, protecting CCL2 against DPP4 cleavage. Therefore, a direct effect of DPP4 on CCL2 seems only possible when large amounts of immature CCL2 are secreted, which might be the case upon strong upregulation of CCL2 protein synthesis. Alternatively, DPP4 (CD26) is important for T cell activation and it has been previously shown that $CCR2^{+}$ T cells are recruited through the choroid plexus to the sides of ischemia (Llovera et al., 2017). Therefore, we speculate that the reduced CCL2 level in DPP4 KO mice might indicate a disturbance of a T cell-regulated CCL2 / CCR2 axis. However, more studies are required to better answer this interesting finding.

We next quantified the cellular responses to reduced CCL2 levels in DPP4 KO mice after stroke by analyzing the activation of astrocytes and of subsets of microglial cells and peripheral MHC-II-positive cells that infiltrated the ischemic brain tissue. We observed an instant activation of astrocytes at 24 h at the ischemic border zone and a delayed activation of Iba1-positive microglial cells at 72 h in the vicinity of the infarction. Intriguingly, the lower post-ischemic CCL2 abundance in DPP4 KO mice was accompanied by diminished Iba1-positive microglial cell activation, compared to WT mice. This is in line with the observations that the DPP4 inhibitor Sitagliptin reduces CCL2 expression and morphologic microglia activation in a model of traumatic brain injury (Hung et al., 2020) and that DPP4 inhibition *in vitro* was shown to reduce the monocyte migration response to CCL2 (Shah et al., 2011). Regarding subsets of microglia cells, the CD68-positive microglia population was unaffected and the MHC-II-positive cells increased during the post-infarct period, whereas the TMEM119-immunoreactive population steadily decreased. This pattern is consistent with TMEM119 being a marker for the homeostatic type of microglia (for reviews see Jurga et al., 2020; Schwabenland et al., 2021).

DPP4 is involved in many physiological processes, including metabolism, neuroendocrinology, the cardiovascular system and the immune system (Klemann et al., 2016; Wagner et al., 2016; Waumans et al., 2015). Thus, the influence of DPP4 on the immune system occurs not only *via* its role in T cell maturation and activation (Klemann et al., 2016), but also *via* the influence of its numerous substrates, which are widely distributed in the central nervous system and involved in many immunomodulatory functions (Wheway et al., 2007). We, therefore, quantified a number of additional chemokines implicated in neuroinflammatory conditions. In our study, CCL5, CCL12 and CCL17 showed higher concentrations in brain tissue or plasma after ischemia, but also lower levels in DPP4 KO compared to WT samples. This is consistent with immunohistochemical data on reduced CCL2 levels in DPP4 KO mice compared to WT mice.

5. Conclusions

Taken together, the DPP4 deficiency in mice improved survival, reduced CCL2 levels and ameliorated microglia activation after induction of experimental stroke. However, the cellular and molecular basis for these effects remain elusive, but could involve memory T cells and T cell-mediated cytokine induction, which is altered by reduced DPP4/CD26 levels.

Ethics approval

All experiments carried out were in agreement with European regulations on the protection of animals used for scientific purposes (Directive 2010/63/EU), and they were also approved by the Ethical Committee for Animal Research of Landesdirektion Sachsen, license number TVV13/18.

Consent for publication

All the authors have approved publication.

CRediT authorship contribution statement

Corinna Höfling: Writing – original draft, Visualization, Validation, Supervision, Methodology, Investigation, Conceptualization. **Philippa Donkersloot:** Validation, Methodology, Investigation. **Luise Ulrich:** Validation, Methodology, Investigation. **Sina Burghardt:** Validation, Methodology, Investigation. **Michael Opitz:** Validation, Methodology, Investigation. **Stefanie Geissler:** Validation, Methodology, Investigation. **Stephan Schilling:** Writing – review & editing, Supervision, Project administration, Funding acquisition, Conceptualization. **Holger Cynis:** Writing – original draft, Project administration, Investigation, Conceptualization. **Dominik Michalski:** Writing – original draft, Validation, Supervision, Methodology, Investigation, Conceptualization. **Steffen Roßner:** Writing – original draft, Supervision, Project administration, Funding acquisition, Conceptualization.

Declaration of competing interest

The authors declare that they have no competing interests.

Data availability

The datasets used and analyzed during the current study are available from the corresponding author on reasonable request.

Acknowledgements

This work was supported by the German Research Foundation (DFG grants #RO 2226/15-1 to SR and #SCHI 1437/2-1 to SS). We thank Eva Jung (Medizinisch-Experimentelles Zentrum, Medical Faculty, Leipzig University) for dedicated pre- and post-surgery animal care and Benjamin Hietel (Fraunhofer IZI-MWT) for excellent technical assistance.

References

Arisi, G.M., Foresti, M.L., Katki, K., Shapiro, L.A., 2015. Increased CCL2, CCL3, CCL5, and IL-1β cytokine concentration in piriform cortex, hippocampus, and neocortex after pilocarpine-induced seizures. J. Neuroinflammation 12, 129.

Baerts, L., Brouns, R., Kehoe, K., Verkerk, R., Engelborghs, S., De Deyn, P.P., Hendriks, D., De Meester, I., 2017. Acute ischemic stroke severity, progression, and outcome relate to changes in dipeptidyl peptidase IV and fibroblast activation protein activity. Transl. Stroke Res. 8, 157–164.

Boehme, A.K., Esenwa, C., Elkind, M.S., 2017. Stroke risk factors, genetics, and prevention. Circ. Res. 120 (3), 472–495.

Chae, Y.N., Kim, T.H., Kim, M.K., Shin, C.Y., Jung, I.H., Sohn, Y.S., Son, M.H., 2015. Beneficial effects of Evogliptin, a novel dipeptidyl peptidase 4 inhibitor, on adiposity with increased Ppargc1a in white adipose tissue in obese mice. PLoS One 10 (12), e0144064.

Chiazza, F., Tammen, H., Pintana, H., Lietzau, G., Collino, M., Nyström, T., Klein, T., Darsalia, V., Patrone, C., 2018. The effect of DPP-4 inhibition to improve functional outcome after stroke is mediated by the SDF-1α/CXCR4 pathway. Cardiovasc. Diabetol. 17 (1), 60.

Choi, S.H., Leem, J., Lee, I.K., 2017. Protective effects of gemigliptin, a dipeptidyl peptidase-4 inhibitor, against cisplatin-induced nephrotoxicity in mice. Mediat. Inflamm. 2017, 4139439.

Darsalia, V., Ortsäter, H., Olverling, A., Darlöf, E., Wolbert, P., Nyström, T., Klein, T., Sjöholm, Å., Patrone, C., 2013. The DPP-4 inhibitor Linagliptin counteracts stroke in the normal and diabetic mouse brain: a comparison with glimepiride. Diabetes 62 (4), 1289–1296.

Darsalia, V., Olverling, A., Larsson, M., Mansouri, S., Nathanson, D., Nyström, T., Klein, T., Sjöholm, Å., Patrone, C., 2014. Linagliptin enhances neural stem cell proliferation after stroke in type 2 diabetic mice. Regul. Pept. 190-191, 25–31.

Darsalia, V., Larsson, M., Nathanson, D., Klein, T., Nyström, T., Patrone, C., 2015. Glucagon-like receptor 1 agonists and DPP-4 inhibitors: potential therapies for the treatment of stroke. J. Cereb. Blood Flow Metab. 35 (5), 718–723.

Darsalia, V., Klein, T., Nyström, T., Patrone, C., 2018. Glucagon-like receptor 1 agonists and DPP-4 inhibitors: anti-diabetic drugs with anti-stroke potential. Neuropharmacology 136 (Pt B), 280–286.
Darsalia, V., Johansen, O.E., Lietzau, G., Nyström, T., Klein, T., Patrone, C., 2019. Dipeptidyl peptidase-4 inhibitors for the potential treatment of brain disorders; a Mini-review with special focus on linagliptin and stroke. Front. Neurol. 10, 493.
Deacon, C.F., Lebovitz, H.E., 2016. Comparative review of dipeptidyl peptidase-4 inhibitors and sulphonylureas. Diabetes Obes. Metab. 18 (4), 333–347.
Durukan, A., Tatlisumak, T., 2007. Acute ischemic stroke: overview of major experimental rodent models, pathophysiology, and therapy of focal cerebral ischemia. Pharmacol. Biochem. Behav. 87 (1), 179–197.
Elmansi, A.M., Awad, M.E., Eisa, N.H., Kondrikov, D., Hussein, K.A., Aguilar-Pérez, A., Herberg, S., Periyasamy-Thandavan, S., Fulzele, S., Hamrick, M.W., McGee-Lawrence, M.E., Isales, C.M., Volkman, B.F., Hill, W.D., 2019. What doesn't kill you makes you stranger: dipeptidyl peptidase-4 (CD26) proteolysis differentially modulates the activity of many peptide hormones and cytokines generating novel cryptic bioactive ligands. Pharmacol. Ther. 198, 90–108.
Esposito, K., Longo, M., Maiorino, M.I., Petrizzo, M., Gicchino, M., Bellastella, G., Giugliano, D., 2019. Metabolic effectiveness of gliflozins and gliptins in the routine clinical practice of patients with type 2 diabetes: preliminary results from GIOIA, a prospective multicentre study. Diabetes Res. Clin. Pract. 155, 107787.
Feigin, V.L., Owolabi, M.O., World Stroke Organization–Lancet Neurology Commission Stroke Collaboration Group, 2023. Pragmatic solutions to reduce the global burden of stroke: a world stroke organization-lancet neurology commission. Lancet Neurol. 22 (12), 1160–1206.
Gilbert, M.P., Pratley, R.E., 2020. GLP-1 analogs and DPP-4 inhibitors in type 2 diabetes therapy: review of head-to-head clinical trials. Front. Endocrinol. (Lausanne) 11, 178.
Gliem, M., Krammes, K., Liaw, L., van Rooijen, N., Hartung, H.P., Jander, S., 2015. Macrophage-derived osteopontin induces reactive astrocyte polarization and promotes re-establishment of the blood brain barrier after ischemic stroke. Glia 63, 2198–2207.
Gliem, M., Schwaninger, M., Jander, S., 2016. Protective features of peripheral monocytes/macrophages in stroke. Biochim. Biophys. Acta 1862, 329–338.
Gyoneva, S., Ransohoff, R.M., 2015. Inflammatory reaction after traumatic brain injury: therapeutic potential of targeting cell-cell communication by chemokines. Trends Pharmacol. Sci. 36 (7), 471–480.
Hartlage-Rübsamen, M., Waniek, A., Meissner, J., Morawski, M., Schilling, S., Jäger, C., Kleinschmidt, M., Cynis, H., Kehlen, A., Arendt, T., Demuth, H.U., Rossner, S., 2015. Isoglutaminyl cyclase contributes to CCL2-driven neuroinflammation in Alzheimer's disease. Acta Neuropathol. 129 (4), 565–583.
Higashijima, Y., Tanaka, T., Yamaguchi, J., Tanaka, S., Nangaku, M., 2015. Anti-inflammatory role of DPP-4 inhibitors in a nondiabetic model of glomerular injury. Am. J. Physiol. Ren. Physiol. 308 (8), F878–F887.
Hung, Y.W., Wang, Y., Lee, S.L., 2020. DPP-4 inhibitor reduces striatal microglial deramification after sensorimotor cortex injury induced by external force impact. FASEB J. 34 (5), 6950–6964.
Ikedo, T., Minami, M., Kataoka, H., Hayashi, K., Nagata, M., Fujikawa, R., Higuchi, S., Yasui, M., Aoki, T., Fukuda, M., Yokode, M., Miyamoto, S., 2017. Dipeptidyl peptidase-4 inhibitor anagliptin prevents intracranial aneurysm growth by suppressing macrophage infiltration and activation. J. Am. Heart Assoc. 6 (6), e004777.
Inose, Y., Kato, Y., Kitagawa, K., Uchiyama, S., Shibata, N., 2015. Activated microglia in ischemic stroke penumbra upregulate MCP-1 and CCR2 expression in response to lysophosphatidylcholine derived from adjacent neurons and astrocytes. Neuropathology 35 (3), 209–223.
Jurga, A.M., Paleczna, M., Kuter, K.Z., 2020. Overview of general and discriminating markers of differential microglia phenotypes. Front. Cell. Neurosci. 14, 198.
Klemann, C., Wagner, L., Stephan, M., von Hörsten, S., 2016. Cut to the chase: a review of CD26/dipeptidyl peptidase-4's (DPP4) entanglement in the immune system. Clin. Exp. Immunol. 185, 1–21.
Kuriyama, N., Mizuno, T., Kita, M., Nagakane, Y., Hosomi, A., Harada, S., Takeda, K., Ozasa, K., Yamada, K., Tokuda, T., Watanabe, Y., Nakagawa, M., 2009. Predictive markers of blood cytokine and chemokine in recurrent brain infarction. J. Interf. Cytokine Res. 29, 729–734.
Lamos, E.M., Hedrington, M., Davis, S.N., 2019. An update on the safety and efficacy of oral antidiabetic drugs: DPP-4 inhibitors and SGLT-2 inhibitors. Expert Opin. Drug Saf. 18 (8), 691–701.
Leung, S.Y., Wong, M.P., Chung, L.P., Chan, A.S., Yuen, S.T., 1997. Monocyte chemoattractant protein-1 expression and macrophage infiltration in gliomas. Acta Neuropathol. 93 (5), 518–527.
Lier, J., Streit, W.J., Bechmann, I., 2021. Beyond activation: characterizing microglial functional phenotypes. Cells 10, 2236.
Lindemann, C., Marschall, V., Weigert, A., Klingebiel, T., Fulda, S., 2015. Smac mimetic-induced upregulation of CCL2/MCP-1 triggers migration and invasion of glioblastoma cells and influences the tumor microenvironment in a paracrine manner. Neoplasia 17, 481–489.
Llovera, G., Benakis, C., Enzmann, G., Cai, R., Arzberger, T., Ghasemigharagoz, A., Mao, X., Malik, R., Lazarevic, I., Liebscher, S., Ertürk, A., Meissner, L., Vivien, D., Haffner, C., Plesnila, N., Montaner, J., Engelhardt, B., Liesz, A., 2017. The choroid plexus is a key cerebral invasion route for T cells after stroke. Acta Neuropathol. 134 (6), 851–868.
Longa, E.Z., Weinstein, P.R., Carlson, S., Cummins, R., 1989. Reversible middle cerebral artery occlusion without craniectomy in rats. Stroke 20 (1), 84–91.
Ma, M., Hasegawa, Y., Koibuchi, N., Toyama, K., Uekawa, K., Nakagawa, T., Lin, B., Kim-Mitsuyama, S., 2015. DPP-4 inhibition with linagliptin ameliorates cognitive impairment and brain atrophy induced by transient cerebral ischemia in type 2 diabetic mice. Cardiovasc. Diabetol. 14, 54.
Marguet, D., Baggio, L., Kobayashi, T., Bernard, A.M., Pierres, M., Nielsen, P.F., Ribel, U., Watanabe, T., Drucker, D.J., Wagtmann, N., 2000. Enhanced insulin secretion and improved glucose tolerance in mice lacking CD26. Proc. Natl. Acad. Sci. USA 97 (12), 6874–6879.
Marso, S.P., Bain, S.C., Consoli, A., Eliaschewitz, F.G., Jódar, E., Leiter, L.A., Lingvay, I., Rosenstock, J., Seufert, J., Warren, M.L., Woo, V., Hansen, O., Holst, A.G., Pettersson, J., Vilsbøll, T., 2016a. Semaglutide and cardiovascular outcomes in patients with type 2 diabetes. N. Engl. J. Med. 375, 1834–1844.
Marso, S.P., Daniels, G.H., Brown-Frandsen, K., Kristensen, P., Mann, J.F.E., Nauck, M.A., Nissen, S.E., Pocock, S., Poulter, N.R., Ravn, L.S., Steinberg, W.M., Stockner, M., Zinman, B., Bergenstal, R.M., Buse, J.B., 2016b. Liraglutide and cardiovascular outcomes in type 2 diabetes. N. Engl. J. Med. 375, 311–322.
McGovern, A., Tippu, Z., Hinton, W., Munro, N., Whyte, M., de Lusignan, S., 2016. Systematic review of adherence rates by medication class in type 2 diabetes: a study protocol. BMJ Open 6 (2), e010469.
Menzies, S.A., Hoff, J.T., Betz, A.L., 1992. Middle cerebral artery occlusion in rats: a neurological and pathological evaluation of a reproducible model. Neurosurgery 31 (1), 100–106.
Mulvihill, E.E., Drucker, D.J., 2014. Pharmacology, physiology, and mechanisms of action of dipeptidyl peptidase-4 inhibitors. Endocr. Rev. 35 (6), 992–1019.
Nauck, M.A., Meier, J.J., Cavender, M.A., Abd El Aziz, M., Drucker, D.J., 2017. Cardiovascular actions and clinical outcomes with glucagon-like peptide-1 receptor agonists and dipeptidyl peptidase-4 inhibitors. Circulation 136 (9), 849–870.
Röhnert, P., Schmidt, W., Emmerlich, P., Goihl, A., Wrenger, S., Bank U, Nordhoff, K., Täger, M., Ansorge, S., Reinhold, D., Striggow, F., 2012. Dipeptidyl peptidase IV, aminopeptidase N and DPIV/APN-like proteases in cerebral ischemia. J. Neuroinflammation 9, 44.
Sarikaya, H., Ferro, J., Arnold, M., 2015. Stroke prevention - medical and lifestyle measures. Eur. Neurol. 73 (3–4), 150–157.
Schuette-Nuetgen, K., Strecker, J.K., Minnerup, J., Ringelstein, E.B., Schilling, M., 2012. MCP-1/CCR-2-double-deficiency severely impairs the migration of hematogenous inflammatory cells following transient cerebral ischemia in mice. Exp. Neurol. 233 (2), 849–858.
Schwabenland, M., Brück, W., Priller, J., Stadelmann, C., Lassmann, H., Prinz, M., 2021. Analyzing microglial phenotypes across neuropathologies: a practical guide. Acta Neuropathol. 142 (6), 923–936.
Shah, Z., Kampfrath, T., Deiuliis, J.A., Zhong, J., Pineda, C., Ying, Z., Xu, X., Lu, B., Moffatt-Bruce, S., Durairaj, R., Sun, Q., Mihai, G., Maiseyeu, A., Rajagopalan, S., 2011. Chronic DPP-4 inhibition reduces atherosclerosis and inflammation via effects on monocyte recruitment and chemotaxis. Circulation 124, 2338–2349.
Shirakawa, J., Fujii, H., Ohnuma, K., Sato, K., Ito, Y., Kaji, M., Sakamoto, E., Koganei, M., Sasaki, H., Nagashima, Y., Amo, K., Aoki, K., Morimoto, C., Takeda, E., Terauchi, Y., 2011. Diet-induced adipose tissue inflammation and liver steatosis are prevented by DPP-4 inhibition in diabetic mice. Diabetes 60 (4), 1246–1257.
Sokolova, A., Hill, M.D., Rahimi, F., Warden, L.A., Halliday, G.M., Shepherd, C.E., 2009. Monocyte chemoattractant protein-1 plays a dominant role in the chronic inflammation observed in Alzheimer's disease. Brain Pathol. 19, 392–398.
Spiteri, A.G., Wishart, C.L., King, N.J.C., 2020. Immovable object meets unstoppable force? Dialogue between resident and peripheral myeloid cells in the inflamed brain. Front. Immunol. 11, 600822.
Sterrett, J.J., Bragg, S., Weart, C.W., 2016. Type 2 diabetes medication review. Am J Med Sci 351 (4), 342–355.
Steven, S., Frenis, K., Oelze, M., Kalinovic, S., Kuntic, M., Bayo Jimenez, M.T., Vujacic-Mirski, K., Helmstädter, J., Kröller-Schön, S., Münzel, T., Daiber, A., 2019. Vascular inflammation and oxidative stress: major triggers for cardiovascular disease. Oxidative Med. Cell. Longev. 2019, 7092151.
Strecker, J.K., Minnerup, J., Gess, B., Ringelstein, E.B., Schäbitz, W.R., Schilling, M., 2011. Monocyte chemoattractant protein-1-deficiency impairs the expression of IL-6, IL-1β and G-CSF after transient focal ischemia in mice. PLoS One 6 (10), e25863.
Strecker, J.K., Minnerup, J., Schütte-Nütgen, K., Gess, B., Schäbitz, W.R., Schilling, M., 2013. Monocyte chemoattractant protein-1-deficiency results in altered blood-brain barrier breakdown after experimental stroke. Stroke 44 (9), 2536–2544.
Ussher, J.R., Drucker, D.J., 2012. Cardiovascular biology of the incretin system. Endocr. Rev. 33 (2), 187–215.
Ussher, J.R., Drucker, D.J., 2014. Cardiovascular actions of incretin-based therapies. Circ. Res. 114 (11), 1788–1803.
Vankriekelsvenne, E., Chrzanowski, U., Manzhula, K., Greiner, T., Wree, A., Hawlitschka, A., Llovera, G., Zhan, J., Joost, S., Schmitz, C., Ponsaerts, P., Amor, S., Nutma, E., Kipp, M., Kaddatz, H., 2022. Transmembrane protein 119 is neither a specific nor a reliable marker for microglia. Glia 70 (6), 1170–1190.
Wafa, H.A., Wolfe, C.D.A., Emmett, E., Roth, G.A., Johnson, C.O., Wang, Y., 2020. Burden of stroke in Europe: thirty-year projections of incidence, prevalence, deaths, and disability-adjusted life years. Stroke 51 (8), 2418–2427.
Wagner, L., Klemann, C., Stephan, M., 2016. von Hörsten S (2016) unravelling the immunological roles of dipeptidyl peptidase 4 (DPP4) activity and/or structure homologue (DASH) proteins. Clin. Exp. Immunol. 184 (3), 265–283.
Wattananit, S., Tornero, D., Graubardt, N., Memanishvili, T., Monni, E., Tatarishvili, J., Miskinyte, G., Ge, R., Ahlenius, H., Lindvall, O., Schwartz, M., Kokaia, Z., 2016. Monocyte-derived macrophages contribute to spontaneous long-term functional recovery after stroke in mice. J. Neurosci. 36, 4182–4195.
Waumans, Y., Baerts, L., Kehoe, K., Lambeir, A.M., De Meester, I., 2015. The dipeptidyl peptidase family, prolyl oligopeptidase, and prolyl carboxypeptidase in the immune system and inflammatory disease, including atherosclerosis. Front. Immunol. 6, 387.

Westin, K., Buchhave, P., Nielsen, H., Minthon, L., Janciauskiene, S., Hansson, O., 2012. CCL2 is associated with a faster rate of cognitive decline during early stages of Alzheimer's disease. PLoS One 7, e30525.
Wheway, J., Herzog, H., Mackay, F., 2007. The Y1 receptor for NPY: a key modulator of the adaptive immune system. Peptides 28, 453–458.
Worthmann, H., Tryc, A.B., Goldbecker, A., Ma, Y.T., Tountopoulou, A., Hahn, A., Dengler, R., Lichtinghagen, R., Weissenborn, K., 2010. The temporal profile of inflammatory markers and mediators in blood after acute ischemic stroke differs depending on stroke outcome. Cerebrovasc. Dis. 30 (1), 85–92.
Yang, D., Nakajo, Y., Iihara, K., Kataoka, H., Yanamoto, H., 2013. Alogliptin, a dipeptidylpeptidase-4 inhibitor, for patients with diabetes mellitus type 2, induces tolerance to focal cerebral ischemia in non-diabetic, normal mice. Brain Res. 1517, 104–113.
Yip, H.K., Lee, M.S., Li, Y.C., Shao, P.L., Chiang, J.Y., Sung, P.H., Yang, C.H., Chen, K.H., 2020. Dipeptidyl peptidase-4 deficiency effectively protects the brain and neurological function in rodent after acute hemorrhagic stroke. Int. J. Biol. Sci. 16 (16), 3116–3132.
Young, A.R., Ali, C., Duretête, A., Vivien, D., 2007. Neuroprotection and stroke: time for a compromise. J. Neurochem. 103 (4), 1302–1309.